

A Low-Noise Superconductive Nb Hot-Electron Mixer at 2.5 THz

B.S. Karasik*, M.C. Gaidis, W.R. McGrath, B. Bumble, and H.G. LeDuc
Center for Space Microelectronics Technology, Jet Propulsion Laboratory,
California Institute of Technology, Pasadena, CA 91109, USA

We report on the development of a quasioptical Nb hot-electron bolometer mixer for a 2.5 THz heterodyne receiver. The devices are fabricated from a 12 nm thick Nb film, and have a $0.30\ \mu\text{m} \times 0.15\ \mu\text{m}$ in-plane size, thus exploiting diffusion as the electron cooling mechanism. The rf coupling was provided by a twin-slot planar antenna on an elliptical Si lens. A specially designed 2.5 THz system, using a CO₂-pumped FIR laser as local oscillator (LO), with rf hot/cold loads enclosed in vacuum to avoid atmospheric absorption, was used in the experiment. The experimentally measured double sideband (DSB) noise temperature of the receiver was as low as $2750 \pm 250\ \text{K}$, with an estimated mixer noise temperature of $\approx 900\ \text{K}$. These results demonstrate the low-noise operation of the diffusion-cooled bolometer mixer above 2 THz.

I. INTRODUCTION

A number of on-going astrophysical and atmospheric programs are aimed at spectroscopic exploration of the terahertz (THz) frequency range. There is an urgent need here for low-noise mixers for heterodyne receivers. Currently available SIS mixers and Schottky-diode mixers exhibit significant degradation in noise performance above 1 THz [1] (see Fig. 1). A unique superconducting hot-electron bolometer (HEB) mixer has been proposed [2-3] as an alternative to address these high-frequency needs. The HEB mixer is expected to operate up to at least several 10's of THz, due to the relatively frequency independent absorption of rf radiation in a superconductor above the gap frequency. Theory [4] predicts the HEB mixer noise temperature due to intrinsic noise mechanisms to be as low as $\sim 100\ \text{K}$, which is of the order of the quantum limit at THz frequencies. Also the required local oscillator (LO) power can be made very low (less than 100 nW for Nb devices) if the device size and sheet resistance are appropriately chosen. Two different approaches have been pursued to develop a practical HEB mixer. The first device approach employs an ultrathin ($< 40\ \text{\AA}$) NbN film where, due to the fast phonon escape, the mixer 3-dB IF signal bandwidth, $f_{3\text{db}}$, is determined by the intrinsic electron-phonon interaction time τ_{ep} to be $f_{3\text{db}} = 1/(2\pi\tau_{\text{ep}}) \approx 3\text{-}4\ \text{GHz}$ [5]. The other major approach utilizes thicker ($\approx 100\ \text{\AA}$) low-resistive high quality Nb films, in which out-diffusion of electrons to normal metal contacts serves as the dominant electron cooling mechanism. For Nb device lengths L less than $0.4\ \mu\text{m}$, useful IF bandwidths have been demonstrated in the range of 2-6 GHz [6-7].

In this work we developed and tested a quasioptical diffusion-cooled HEB mixer at 2.5 THz. Record sensitivity was obtained at this frequency demonstrating the superiority of HEB mixers at THz frequencies.

II. MIXER DESIGN AND EXPERIMENTAL SET-UP

The bolometer device used in this experiment consists of a $0.30\ \mu\text{m}$ long by $0.15\ \mu\text{m}$ wide

* Electronic mail: karasik@merlin.jpl.nasa.gov

microbridge made of a 12 nm thick Nb film sputtered-deposited on a high-resistivity ($\rho \approx 4\text{-}5 \text{ k}\Omega \text{ cm}$) silicon substrate. The length of the bridge was defined by the gap between the 150 nm thick gold contact pads using a unique self-aligned fabrication process [8]. The surrounding mixer embedding circuit and planar antenna are fabricated from 300 nm thick gold. This process gives automatic registration of the Nb under the gold to provide dependable electrical and thermal contact. Figure 2 shows an SEM of a completed device. To protect the device against oxidation the entire area surrounding the microbridge was passivated with a 40 nm thick layer of SiO. More details of the device fabrication are given elsewhere [8]. The critical temperature of the film was 6.8 K, the transition width was 0.2-0.3 K, and the sheet resistance was 11-13 Ω/sq . After patterning of the device, the critical temperature decreased typically to 6.5 K without significant change of other film parameters. The critical current density at 4.2 K was measured to be $1.5 \times 10^7 \text{ A/cm}^2$.

The mixer rf embedding circuit was made using a twin-slot antenna and coplanar waveguide transmission (CPW) line [9] located at the second focus of an elliptical Si lens of 12.7 mm diameter [10]. Figure 3 shows this planar circuit. Our antenna design uses a slot length of 36.5 μm , a slot width of 2.0 μm , and a center-to-center slot spacing of 19.0 μm . A $Z_0 = 39 \Omega$ CPW feed connects to the HEB, with center strip width of 2.0 μm and gaps of 0.5 μm each. The rf impedance presented to the HEB device at the feed point was designed to be 70 Ω , and was strongly determined by the 0.5 μm gap in the CPW line. The IF and dc line integrates an rf choke with 4 high- and 4 low-impedance CPW sections each of 12 μm length. The (85 Ω) high-impedance sections have center strip widths of 1.0 μm and gaps of 4 μm each. The (34 Ω) low-impedance sections have center strip widths of 7.0 μm and gaps of 1 μm each. A 250 μm thick Si chip carrying the twin-slot antenna and rf choke-filter was glued to the lens and wire-bonded to a coplanar waveguide IF circuit on DuroidTM substrate which, in turn, was soldered to an SMA connector.

Our mixer test system (see Fig. 4) consisted of a CO₂-pumped methanol FIR laser as an LO source, and a vacuum box containing two blackbody loads with similar emissivities for Y-factor measurements of the receiver noise temperature. The box is connected to the LHe vacuum cryostat, allowing operation without a pressure window in the signal path. The box and cryostat are evacuated to remove the effect of atmospheric absorption which is significant at 2.5 THz. Thus accurate measurements of receiver noise are possible without any corrections applied. We use a 200 μm thick ZitexTM G108 [11] infrared filter to block background 300 K radiation. The LO beam was diplexed into the signal path using a 12.7 μm thick Mylar beam splitter. One of the blackbody loads was attached to the cold finger of a liquid N₂ dewar and reached a temperature of typically 90 K. The signal from the hot and cold loads was switched by a mechanical chopper with a reflecting blade at a rate typically around 100 Hz. The first-stage of the IF system consisted of a cooled broadband HEMT amplifier with a bandwidth 1.5-3.0 GHz and a noise temperature of ≈ 9 K. This was followed by room-temperature amplifiers, a narrow bandpass filter (a set of different filters with bandwidths ranging from 25 to 300 MHz was used), and a commercial crystal detector. The average IF response, V_{dc} , (*i.e.*, the dc voltage across the IF crystal detector) and the change in IF response synchronous with the chopper, ΔV , were simultaneously measured using a voltmeter and a lock-in amplifier. The Y-factor is then given by $(V_{dc} + \Delta V/2)/(V_{dc} - \Delta V/2)$, and the DSB mixer noise temperature, T_M , is $T_M = (T_H - T_C Y)/(Y - 1)$, where T_H and T_C are the effective Planck temperatures of the hot and cold loads.

III. EXPERIMENTAL PROCEDURE

A. RF Antenna and Coupling Test.

The antenna frequency response was measured using a Fourier Transform Spectrometer (FTS). For this measurement, the device operating temperature was set to a value near T_c , and the bias voltage was adjusted to obtain a large direct-detection response in the bolometer. The detector response was corrected

for the calculated frequency dependence of the beamsplitter in the spectrometer. The remaining frequency dependence is dominated by the antenna response. From the result shown in Fig. 5(A), the center frequency is about 1900 GHz and the 3-dB bandwidth is approximately 1.1 THz. These results conform with the expected performance for twin-slots [9] and demonstrate that this type of antenna functions well above 2 THz. Previously, twin-slot antennas have been successfully demonstrated only slightly above 1 THz [12].

One can see that the center frequency was offset by almost 25% from the desired 2.5 THz center frequency. We have investigated the antenna rf performance, attempting to understand this discrepancy with the 2.5 THz design. A detailed model simulation revealed a significant dependence of center frequency on the HEB device resistance. Figure 5(B) shows the result of simulations for 3 different device resistances. The antenna was designed to provide a match to a 70 Ω HEB with a 2.5 THz center frequency. The 23 Ω HEB device, actually tested as a mixer, would be expected to best match the antenna at about 2.25 THz which is only 18% higher than the experimental result. To examine these issues further, we have tested a 35 Ω device with the same antenna design as used for the previous 23 Ω device. In this case, we find the theory is about 7% higher than the measured center frequency. We have not yet been able to test more devices of this type on the FTS to evaluate the statistical significance of this deviation, but find it to be quite close to the errors one could expect from the theoretical model simulations. Tests with more devices of varying resistances will also reveal the significance of the device resistance on match to theory. The rf choke filter was assumed ideal in the simulations, but may also play a role in the observed discrepancy. The first rf filter section presented to the antenna is a low-impedance section which flares at 45° to match the dimensions of the CPW inside the twin-slot antenna. One other 49 Ω device tested with a modified rf filter in which the first section does not have the 45° flare, showed less than 1% deviation from theory, but the lack of more tests prevents us from yet concluding that the rf choke is responsible for the 7-18% shift seen above. It is also likely that the Zitex G108 or G115 IR filters used in the experiment causes a small downshift, as it exhibits a rolloff beginning only slightly above 2.5 THz. The Zitex is responsible for the deviation between the calculated and measured response above 3 THz. Finally it is useful to note that the theory predicts approximately 1.5 dB of loss at the LO frequency of 2.522 THz for the 23 Ω , whereas the FTS measurements suggest up to 3 dB improvement may be possible for an optimized device/antenna combination.

The coupling efficiency of the bolometer to the radiation (which includes all the losses and reflections in the warm and cold optics, as well as embedding circuit losses) was measured using the direct detection response of the HEB to the hot and cold loads (*i.e.*, without any LO applied). Plotting the two current-voltage (IV) characteristics (“hot” and “cold”) one can calculate the absorbed radiation power, P_{abs} , assuming the rf power heats the device in the same fashion as the dc bias Joule heating. Here, $P_{\text{abs}} = P_{\text{dc}}(\text{hot}) - P_{\text{dc}}(\text{cold})$, applied for a constant resistance line (P_{dc} is the Joule power). The device coupling efficiency can be found as $\eta = P_{\text{abs}}/\Delta P_{\text{inc}}$, where ΔP_{inc} is the difference between the powers of black body radiation from the hot and cold loads, integrated over the measured rf bandwidth of the mixer. This yields a total optical coupling efficiency of $\eta \approx -7.2$ dB.

B. Y-factor and LO power.

Mixer experiments were performed with two very similar devices, and both demonstrated comparable performance. Only the data for one are discussed here. Figure 6 shows both unpumped and optimally LO-pumped IV characteristics at 4.3 K. Normally, only small or no negative resistance was observed in the optimal IV curve. The LO power (P_{lo}) absorbed in the bolometer was evaluated from the pumped and unpumped IV characteristics as $P_{\text{lo}} = P_{\text{dc}}(\text{unpumped}) - P_{\text{dc}}(\text{pumped})$, applied for a constant resistance line. Within the uncertainty of this simple technique, $P_{\text{lo}} \approx 80$ nW was obtained. In addition, special precautions have been taken (including very careful alignment, absorbers to catch stray reflections, and aperturing of the laser beam) to reduce reflections and LO standing wave effects to a negligibly small

level. This was required to obtain a stable ac component ΔV for Y-factor measurements. Also the offset of the output noise caused by the direct detection of the THz radiation within the antenna bandwidth was verified as too small to contribute significantly to the observed mixing signals. In particular, we have checked that the highest possible IF noise offsets caused by the direct detection at different temperatures (LO power turned off) were still much smaller than the mixing response.

The bias dependencies of both V_{dc} and ΔV are given in the same figure. One can see that the IF output power starts to rise when approaching the dropback point at the IV curve, indicating the onset of strong mixing performance (at this point the dynamic resistance becomes very large and the self-heating effects increase). This behavior was also observed at 1.5 K, where both the position of the operating point and the mixer noise temperature were almost the same as at 4.3 K. The only difference was a somewhat larger amount of LO power required to pump the mixer at 1.5 K. Also, for bias voltages in the negative differential resistance region, the generation of oscillations in the device were observed. This bias region was avoided for mixer measurements.

C. IF Impedance and Mixer Bandwidth.

In order to estimate the IF bandwidth inherent in the mixer device we performed IF impedance measurements within a 0.05-4 GHz frequency range. It has been demonstrated experimentally for phonon-cooled Nb [13,14] and NbN [15] devices that the HEB impedance changes from a high differential resistance value at low frequencies to a lower ohmic resistance R at high frequencies. The crossover occurs at the frequencies related to the intrinsic electron temperature relaxation time, τ_T . Thus, a measurement of the HEB impedance versus frequency allows τ_T to be determined. The mixer bandwidth, f_{3dB} , is then given by:

$$f_{3dB}^{-1} = \frac{\tau_T}{1 + C \frac{R - R_L}{R + R_L}}, \quad (1)$$

where R_L is the IF load (50 Ω), and C is the self-heating parameter.

For these measurements, a 0.3 μm long device with small contact pads was mounted in a gap in the center conductor of a microstrip transmission line fabricated on 0.5 mm thick Duroid with dielectric constant 10.2. The line was placed in a dewar and connected through semirigid cables with a HP8510 network analyzer to measure the S_{21} parameter. The testing rf power level was greatly attenuated to avoid any influence of the test signal on the device resistive state. Calibrations were done with the HEB device in the superconductive state ($Z \approx 0$) and normal state ($Z = R_n$). This allowed the HEB IF impedance to be de-embedded from the microstrip test fixture. According to theory [4] the HEB impedance is given by

$$Z(\omega) = R \frac{1 + C}{1 - C} \frac{1 + j\omega \frac{\tau_T}{1 + C}}{1 + j\omega \frac{\tau_T}{1 - C}}. \quad (2)$$

Large values of the parameter C are required in order to observe a pronounced frequency dependence of the impedance. Equivalently, the device has to be biased to the operating point with a large differential resistance. In the experiment this was accomplished by heating the device to some temperature above 4.2 K. Figure 7 shows the IV curve and the position of the operating point for these measurements. Figure 8 shows the $Z(f)$ dependence (both real and imaginary parts) along with the fitted curves from Eq. 2. The associated mixer bandwidth is found to be $f_{3dB} = 1.4$ GHz. This quantity is in good agreement with recently reported bandwidth measurements on diffusion-cooled Nb devices of the same length [6,7].

IV. NOISE TEMPERATURE AND LOSSES

The experimental values of the DSB receiver noise temperature are plotted vs IF in Fig. 9. The different points correspond to the different bandpass filters used. A best receiver noise of 2500-3000 K was measured at IF's below 1.4 GHz, *i.e.* the noise bandwidth is consistent with the mixer bandwidth implied by the impedance measurements. If we remove the IF system noise and correct for the measured 1.5-dB loss in the off-resonant antenna, an upper limit of about 900 K is obtained for the mixer noise temperature. This performance is comparable to that for similar diffusion-cooled HEB mixers at 533 GHz [6] and at 1.2 THz [16], and demonstrates the relative frequency-independence of the mixer performance. It should be noted that this receiver performance is 3-to-5 times better than competing Schottky-diode receivers at 2.5 THz, and the required LO power is at least four orders of magnitude lower.

TABLE I
BALANCE OF THE RECEIVER LOSSES

Element	Loss (dB)
Si lens (reflection)	1.5
Si lens (absorption)	<0.3
Beamsplitter	0.5
Zitex filter	≤0.5
Mixer center frequency offset	3.0
Twin-slot antenna backlobe loss	0.5
CPW conduction losses	1.0
TOTAL:	7.3

We believe that this measured performance, while very good, is certainly not the best possible for an optimized device. Table I shows a loss budget at the mixer rf path. One can estimate that the DSB noise temperature at the device itself (after eliminating the 7.3 dB rf loss) may be as low as ≈ 500 K. Such corrections always involve substantial uncertainty, but at least are indicative of the noise performance of this type of HEB mixer. In addition, a better optimized design of the antenna circuit and use of an appropriate anti-reflection coating for the Si lens can reduce the receiver noise temperature to below 1000 K.

V. CONCLUSION

Excellent performance of a diffusion-cooled Nb hot-electron bolometer mixer has been demonstrated at 2.5 THz. A DSB receiver noise temperature of ≤ 3000 K has been measured at $f_{IF} \leq 1.4$ GHz, along with only 80 nW coupled LO power. The mixer performance is expected to improve by at least 1.5-2 dB with better antenna design and impedance match. This demonstrates that diffusion-cooled HEB mixers can work up above 2 THz with no significant degradation in performance. This is a major improvement for heterodyne sensor technology and is expected to be extremely useful for numerous astrophysical and atmospheric applications.

ACKNOWLEDGMENT

The authors are thankful to A. Skalare for numerous discussions and valuable contributions during set up of the experiment, G. Rebeiz for calculation of the twin-slot antenna and J. Zmuidzinas for the use of his computer program to model the twin-slot antenna impedance. M. Shumate is acknowledged for setting up the FIR laser. We also acknowledge T. Crawford and H. Pickett for the use of FTS and assistance with the measurements.

The research described in this paper was performed by the Center for Space Microelectronics Technology, Jet Propulsion Laboratory, California Institute of Technology, and was sponsored by the National Aeronautics and Space Administration, Office of Space Science.

REFERENCES

- [1] These data are borrowed from different sources: Schottky diode data are taken from the Proc. 7th Int. Symp. on Space Terahertz Technology (STT-7), University of Virginia, Charlottesville, VA, March 1996; most recent SIS data are from STT-7 and Ref. 11; NbN HEB data are from STT-6, STT-7, Ref. 5, J. Kawamura et al., *J. Appl. Phys.*, vol. 80, pp. 4232-4234, October 1996; *Appl. Phys. Lett.*, vol. 70, March 1997, and A.D. Semenov et al. *Appl. Phys. Lett.*, vol. 69, pp. 260-262, July 1996; Nb HEB data are from Ref. 6,16 and this work.
- [2] E.M. Gershenzon, G.N. Gol'tsman, I.G. Gogidze, Y.P. Gusev, A.I. Elant'ev, B.S. Karasik, and A.D. Semenov, "Millimeter and submillimeter range mixer based on electronic heating of superconducting films in the resistive state," *Sverhprovodimost' (KIAE)*, vol. 3(10), pp. 2143-2160, October 1990 [*Sov. Phys. Superconductivity*, vol. 3(10), pp. 1582-1597, 1990];
- [3] D.E. Prober, "Superconducting terahertz mixer using a transition-edge microbolometer," *Appl. Phys. Lett.* vol. 62(17), pp. 2119-2121, 26 April 1993.
- [4] B.S. Karasik and A.I. Elantiev, "Noise temperature limit of a superconducting hot-electron bolometer mixer," *Appl. Phys. Lett.*, vol. 68, pp. 853-855, February 1996; "Analysis of the noise performance of a hot-electron superconducting bolometer mixer," *Proc. of the 6th Int. Symp. on Space Terahertz Technology*, 21-23 March 1995, Caltech, Pasadena, pp. 229-246.
- [5] P. Yagubov, G. Gol'tsman, B. Voronov, S. Svechnikov, S. Cherednichenko, E. Gershenzon, V. Belitsky, H. Ekström, E. Kollberg, A. Semenov, Yu. Gousev, and K. Renk, "Quasioptical phonon-cooled NbN hot-electron bolometer mixer at THz frequencies," *Proc. 7th Int. Symp. on Space Terahertz Technology*, University of Virginia, Charlottesville, VA, March 1996, pp. 303-317.
- [6] A. Skalare, W.R. McGrath, B. Bumble, H.G. LeDuc, P.J. Burke, A.A. Verheijen, R.J. Schoelkopf, and D.E. Prober, "Large bandwidth and low noise in a diffusion-cooled hot-electron bolometer mixer," *Appl. Phys. Lett.*, vol. 68, pp. 1558-1560, March 1996.
- [7] P.J. Burke, R.J. Schoelkopf, D.E. Prober, A. Skalare, W.R. McGrath, B. Bumble, and H.G. LeDuc, "Length scaling of bandwidth and noise in hot-electron superconducting mixer," *Appl. Phys. Lett.*, vol. 68, pp. 3344-3346, June 1996.
- [8] B. Bumble and H.G. LeDuc, "Fabrication of a diffusion cooled superconducting hot electron bolometer for THz mixing applications", *IEEE Transactions on Applied Superconductivity*, vol. 7, pp.3560-3563, June 1997.
- [9] D.F. Fillipovic, S.S. Gearhart, G.M. Rebeiz, "Double-slot antennas on extended hemispherical and elliptical silicon dielectric lenses," *IEEE Trans. on Microwave Theory and Technique*, vol. 41, pp. 1738-1749, October 1993.
- [10] The Si lenses have been fabricated at Janos Technology Inc., Townshed, VT 05353-7702.
- [11] Zitex G108, Norton Performance Plastics, Wayne, NJ 07470-4699.
- [12] M. Bin, M.C. Gaidis, J. Zmuidzinas, T.G. Phillips, and H.G. LeDuc, "Low-noise 1 THz niobium superconducting tunnel junction mixer with a normal metal tuning circuit," *Appl. Phys. Lett.*, vol. 68, pp. 1714-1716, March 1996.
- [13] A.I. Elantev and B.S. Karasik, "Effect of high frequency current on Nb superconductive film in the resistive state," *Fiz.Nizk.Temp.*, vol. 15, pp. 675-683 (1989) [*Sov. J.Low Temp. Phys.* vol. 15, pp. 379-383 (1989)].
- [14] H. Ekström, B.S. Karasik, E. Kollberg, K.S Yngvesson, "Superconducting bolometric mixers," *IEEE Trans. Microwave and Guided Wave Letters*, vol. 4, pp. 253-255 (1994).

- [15] H. Ekström, B.S. Karasik, E. Kollberg, G.N. Gol'tsman, and E.M. Gershenzon, "350 GHz hot electron bolometer mixer," *Proc. of the 6th Int. Symp. on Space Terahertz Technology*, 21-23 March 1995, Caltech, Pasadena, pp. 269-283.
- [16] A. Skalare, W.R. McGrath, B. Bumble, H.G. LeDuc, "Receiver measurements at 1267 GHz using a diffusion-cooled superconducting transition-edge bolometer", *IEEE Transactions on Applied Superconductivity*, vol.7, pp. 3568-3571, June 1997; and this conference issue.

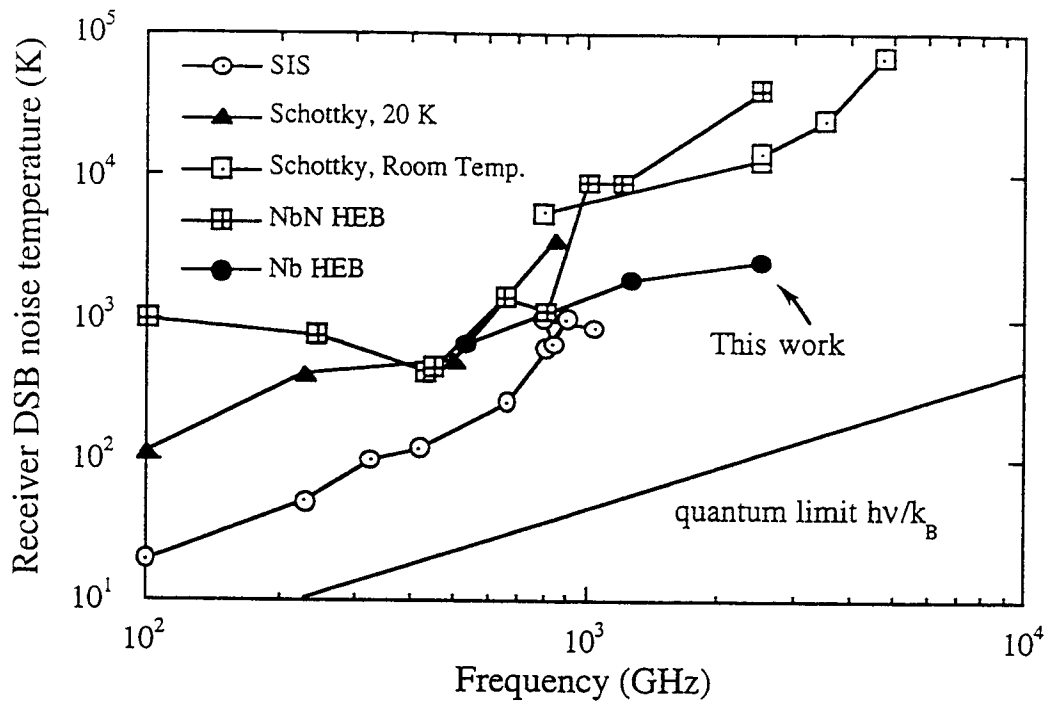


Fig. 1. State-of-the-art in heterodyne receiver noise performance at submillimeter wavelengths.

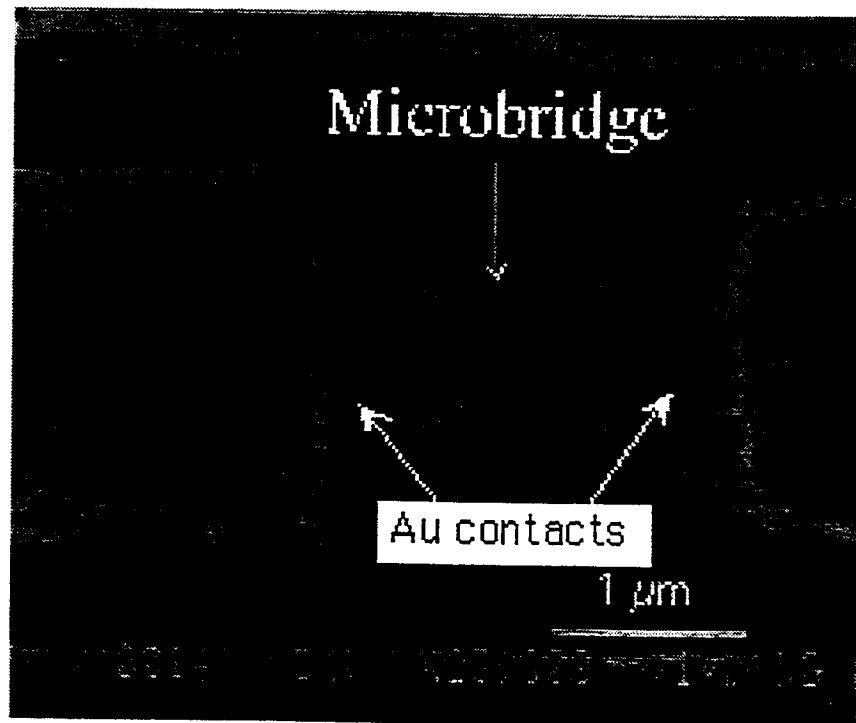


Fig. 2. SEM photo of the 0.30 μm by 0.15 μm Nb HEB device between the gold contacts.

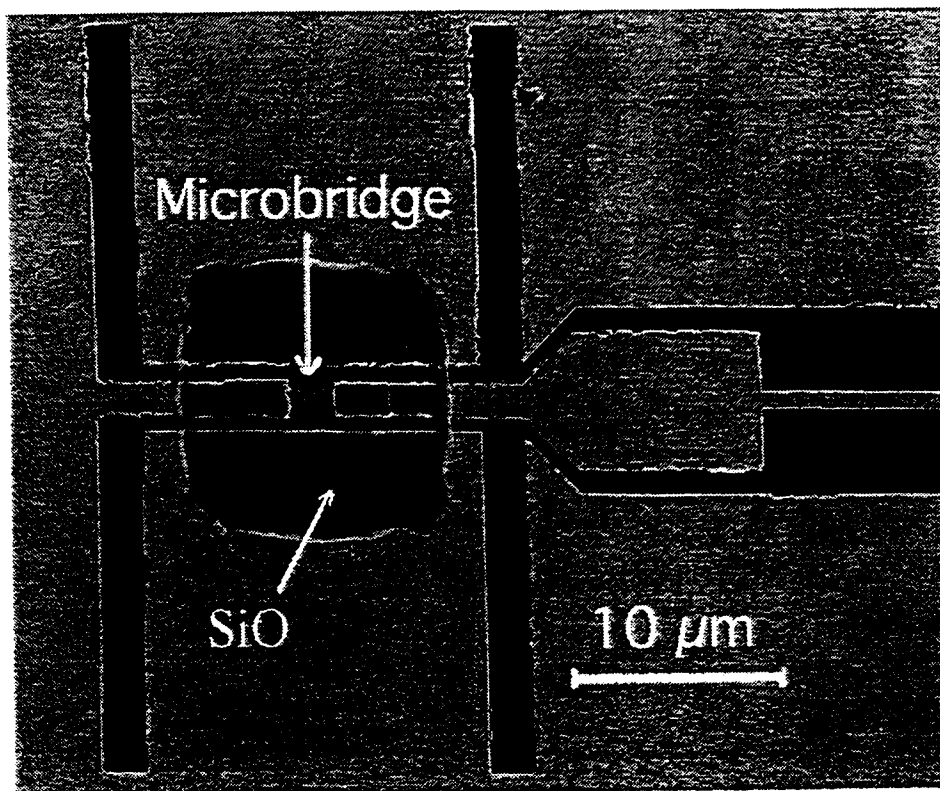


Fig. 3. Photo of the planar mixer circuit consisting of the twin-slot antenna and coplanar waveguide transmission line. The circuit elements to the right are the IF and dc lines with an integrated if choke filter.

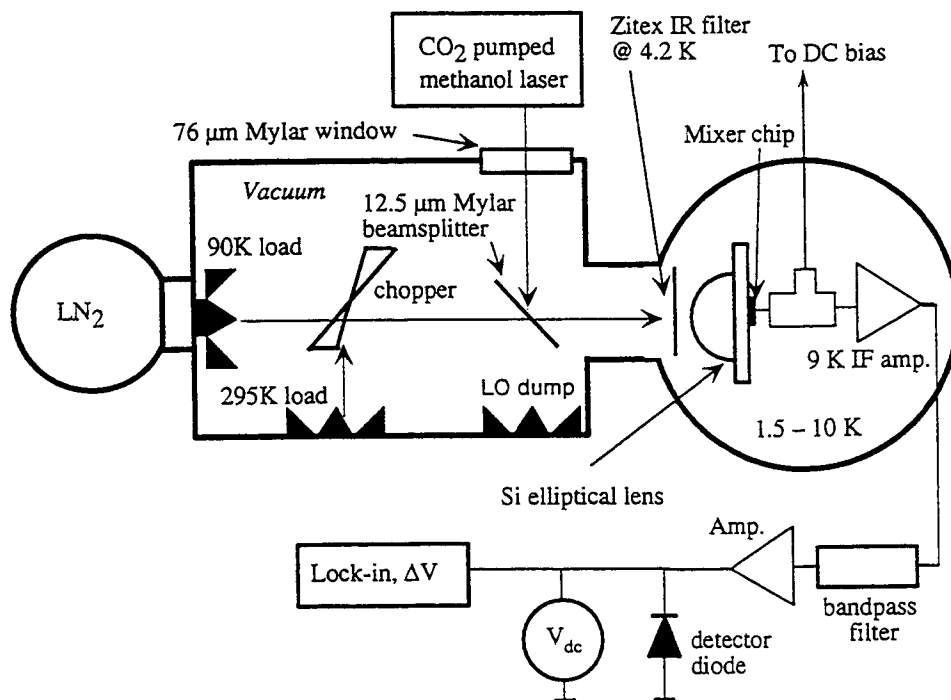


Fig. 4. Block diagram of the 2.5 THz mixer/receiver test system.

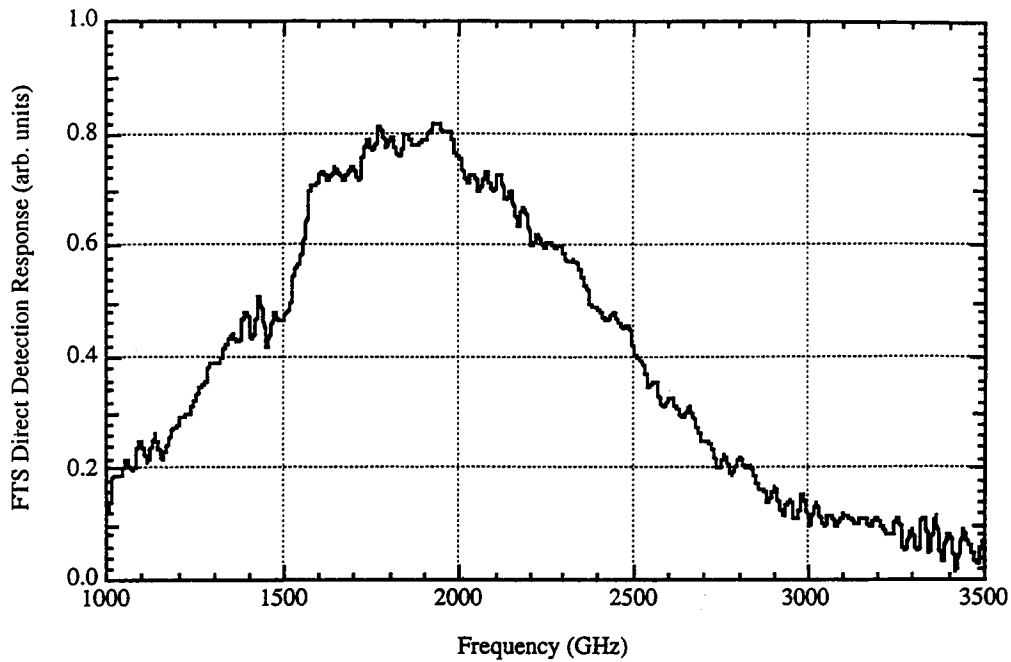


Fig. 5(A). FTS spectrum measured for the 23 Ω HEB, corrected for the calculated 23 μm FTS beamsplitter efficiency. The HEB was operated as a direct detector. The frequency response is determined mainly by the planar antenna and shows that the twin-slot circuit works well at terahertz frequencies.

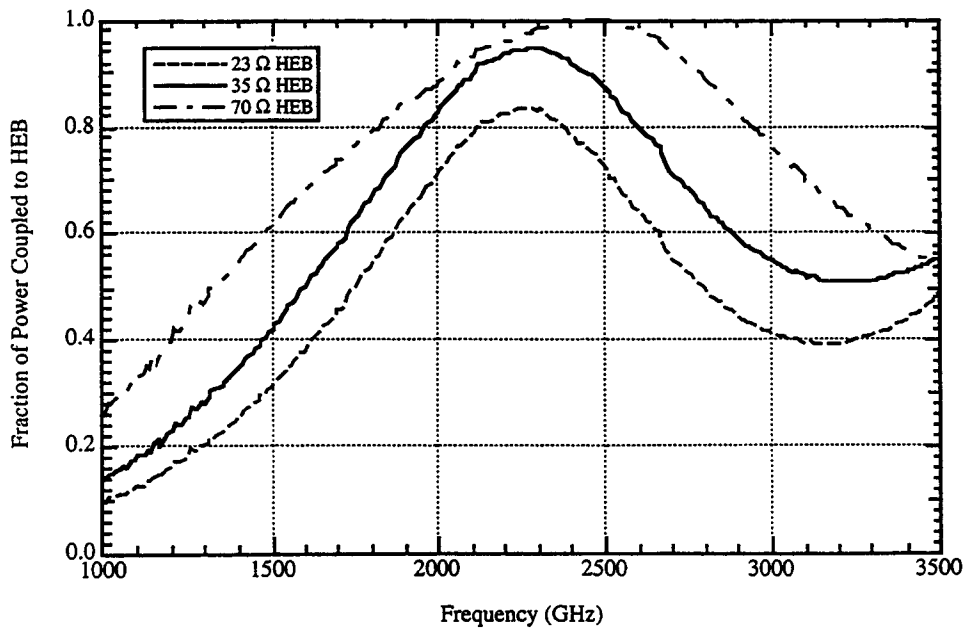


Fig. 5(B). Coupling efficiency of twin-slot antenna and coplanar waveguide to the HEB, calculated for 23 Ω , 35 Ω , and the ideal 70 Ω device resistance.

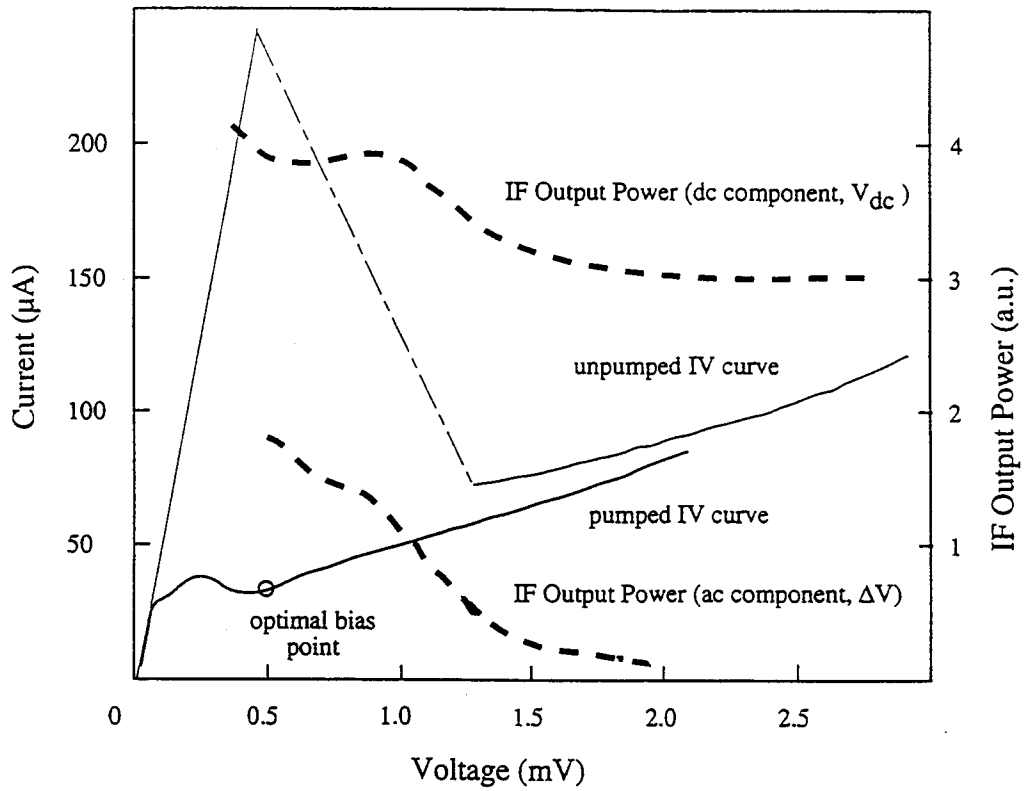


Fig. 6. Current-voltage characteristics and the dc (V_{dc}) and ac (ΔV) components of the IF output power. V_{dc} and ΔV are arbitrary scaled in reference to each other.

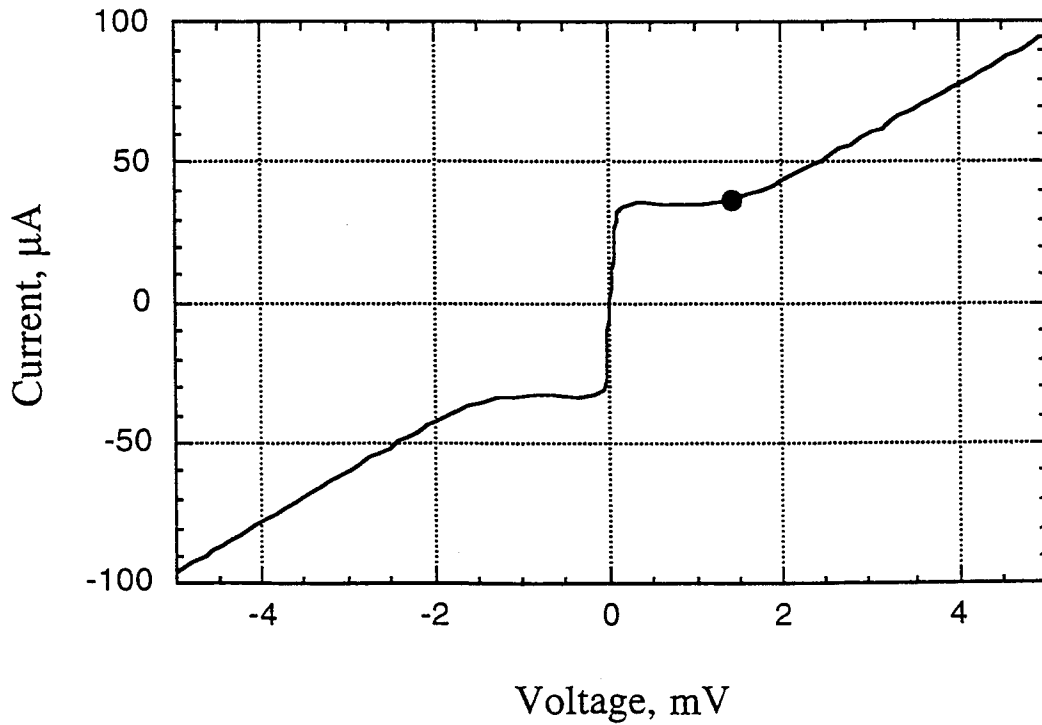


Fig. 7. The IV characteristic and the position of the operating point (filled circle) for the impedance measurements.

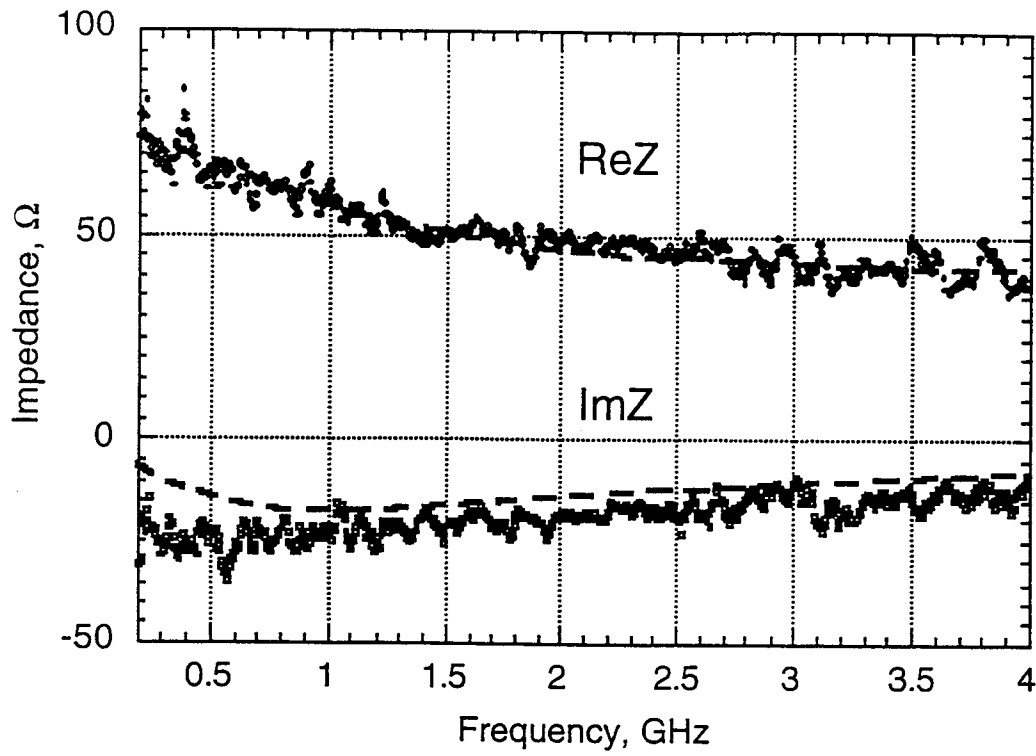


Fig. 8. HEB IF impedance for a $0.3 \mu\text{m}$ long microbridge. The dashed lines are the fit by Eq. 2 with $C = 0.3$

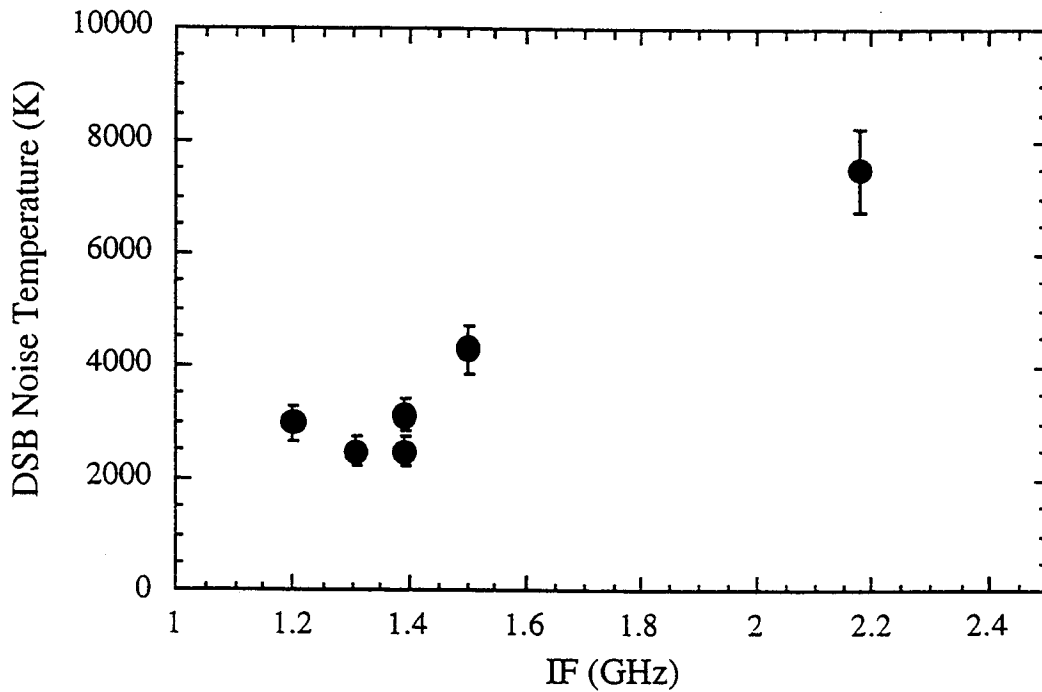


Fig. 9. The receiver noise temperature vs intermediate frequency.